Macrophage fusion leading to foreign body giant cell formation persists under phagocytic stimulation by microspheres in *in vitro* and *in vivo* in mouse models

Steven M. Jay[1,3], **Eleni A. Skokos**[2,3], **Jianmin Zeng**[2,3], **Kristin Knox**[1], and **Themis R. Kyriakides**[1,2,3,*]

[1] Department of Biomedical Engineering, Yale University

[2] Department of Pathology, Yale University

[3] Interdepartmental Program in Vascular Biology and Therapeutics, Yale University

Abstract

The formation of surface-damaging foreign body giant cells (FBGC) from the fusion of macrophages is considered a hallmark of the foreign body response. Experimental evidence indicates that when macrophages are unable to internalize foreign bodies via phagocytosis due to their large size, they acquire a fusogenic phenotype. The mechanism behind this transformation is unclear, and questions, such as which phenotype takes precedence for co-stimulated macrophages engaged in the foreign body response and whether or not such phenotypic alteration is graded, remain unanswered. By recapitulating fusion *in vitro* using cell lines and primary mouse bone marrow-derived macrophages, we investigated whether concurrent exposure of macrophages to phagocytic and fusogenic stimuli would limit fusion. Induction of phagocytosis by addition of 3.0 μm-diameter polystyrene microspheres to cells under fusogenic conditions, at ratios of 1:10, 1:1, and 10:1 did not prevent fusion. To determine the effect of microsphere phagocytosis on fusion *in vivo*, we first determined the kinetics of monocyte recruitment, surface adhesion, and fusion following intraperitoneal implantation of a foreign body in a mouse model. Concomitant or subsequent injection of microspheres resulted in their significant accumulation at the biomaterial surface at 2 weeks, but FBGC were still detected. Our findings indicate that despite increasing the abundance of a phagocytic stimulus (microspheres), significant FBGC formation occurs.

INTRODUCTION

Implanted biomaterials are subject to a significant reaction from the host organism, known as the foreign body response (FBR). During this process, implants are surrounded by macrophages that fuse to form foreign body giant cells (FBGC), as well as a collagenous and largely avascular fibrotic capsule [1,2]. The presence of FBGC at the surface of an implanted material is considered a hallmark of the FBR, and the damaging effects of these cells can lead to reduced functionality or failure in implants [3–5]. Furthermore, FBGC are believed to contribute to the persistence of pro-inflammatory stimuli integral to the FBR [6].

[*]Corresponding author: Themis Kyriakides, Ph.D., Yale University, Department of Pathology, Amistad Building 301C, 10 Amistad St., New Haven, CT 06520.

Despite their significant role in the host response to implanted devices, the cause and mechanism of FBGC formation in this context are not fully understood [1,6,7]. Phenomenological observations suggest that when macrophages adhere to a surface that is too large to be degraded effectively via phagocytosis, they become fusogenic [6,7]. This behavior implies a direct and perhaps linear determination of macrophage functional fate between phagocytosis and fusion. However, this phenomenon has yet to be systematically evaluated, leaving questions, such as whether the functional change from a phagocytic state to a fusogenic one is graded or the result of a physiologic switch, unanswered.

Although the mechanism remains unclear, a relationship between fusion and phagocytosis has been established. Anderson and colleagues showed that macrophage fusion induced by interleukin-4 (IL-4) is dependant on activity of the mannose receptor, a classical phagocytic mediator [8], though it should be noted that phagocytosis in macrophages can be mediated by a number of different mechanisms [9,10]. Furthermore, this group has established extensive homology between phagocytosis and fusion in endoplasmic reticulum function [11] response to vitronectin expression [12], and downstream kinase signaling activity [13]. Others have shown that FBGC can engulf large foreign bodies in a phagocytic-like manner [14] and that macrophages that have phagocytosed particles are capable of fusion in the context of osteoclastic differentiation [15]. However, despite these many similarities, phagocytosis and fusion are distinct processes. In fact, we have shown that fusion and phagocytosis could be partially decoupled based on their differential susceptibility to Rac1 inhibition [16]. Specifically, unlike fusion, phagocytosis, induced by polystyrene microspheres, was shown to be unaffected by blockade of Rac1 activation [16]. In other words, in this model, inhibition of fusion does not necessitate inhibition of phagocytosis.

In order to further understand the decoupling of these processes in the FBR, we sought to develop a correlative model whereby *in vitro* observations could be compared to a clinically relevant *in vivo* biomaterial implant model. A number of *in vitro* fusion assays that utilize monocytes/macrophages from various sources have been developed [17–19]. Recently, we described a system for FBGC formation *in vitro* from mouse bone marrow-derived macrophages using an IL-4 mediated process [16]. In this study, we investigated the potential of using immortalized cell lines in this model, owing to their relatively low cost, ease of procurement, length of maintenance in culture, and prevention of animal sacrifice or need for human donors. For *in vivo* studies, we utilized an established murine model with a cellulose filter serving as a model biomaterial [3,20]. We quantified the kinetics of macrophage recruitment in this model to better understand when fusion might occur *in vivo* so that we could establish correlation with our *in vitro* system.

With a correlative model, this study examined the potential decoupling of phagocytosis and fusion in macrophages during the FBR. We hypothesized that concurrent, profuse induction of phagocytosis by microspheres and fusion via IL-4 would force a determination of cellular fate that might provide further information about the distinguishing features of these two processes. In a mouse bone marrow derived-macrophage model (BMM) *in vitro*, we show that the functional change between microsphere-induced phagocytosis and IL-4 induced-fusion for macrophages is graded in response to increasing phagocytic challenge. However, even with abundant presence of microsperes, substantial FBGC formation still occurs. This effect was also observed *in vivo* in a mouse model, suggesting that, in the FBR, these processes may be more functionally independent than previously thought.

MATERIALS AND METHODS

In vitro fusion assay and phagocytosis

Murine macrophage cell lines RAW264.7 and J7746b, graciously provided by Dr. Agnes Vignery, and human monocyte cell lines THP-1 and U937, generously donated by Dr. Ira Mellman, were cultured in RPMI + 10% FBS with penicillin/streptomycin and l-glutamine. BMM were obtained from the bone marrow of C57Bl/6 mice and expanded as described previously [16]. To recapitulate fusion *in vitro*, various macrophage cell lines (1×10^5 cells/ well) and BMM (1×10^6 cells/well) were plated on 24-well non-tissue culture treated polystyrene plates (Corning, Corning, NY) in expansion media containing 10 ng/ml recombinant human or mouse granulocyte/macrophage-colony stimulating factor (GM-CSF) (R&D Systems, Minneapolis, MN) and 10 ng/ml human or IL-4 (mouse recombinant, R&D Systems, Minneapolis, MN), as described previously [16]. Phagocytosis was stimulated via addition of 3.0 μm-diameter Fluoresbrite YG polystyrene microspheres (Polysciences, Warrington, PA) at microsphere to cell ratios of 1:10, 1:1, and 10:1, as noted. These ratios were chosen to stimulate a small percentage of cells to phagocytose (1:10), provide enough stimulation for most cells to engage in phagocytosis (1:1) and to saturate the phagocytic capacity of the macrophages (10:1) based on studies that indicate that a single macrophage in culture can maximally phagocytose ~4 3.0 μm-diameter beads [21]. Similarly, 3.0 μm-diameter microparticles were chosen based on previous studies indicating that 3.0 μm is an ideal diameter to maximize uptake by macrophages both *in vitro* and *in vivo* [22,23]. To inhibit Rac1 activation, cultures containing fusogenic stimuli and/or microspheres were treated with 25μM NSC23766 (Calbiochem, La Jolla, CA) and phagocytosis and fusion were measured as described previously [24]. Experiments involving cell lines were performed in triplicate wells and performed three times. For each experiment with BMM, monocytes were isolated from 6 femurs (three mice), expanded and pooled and triplicate wells were prepared for each condition and time point. Experiments were repeated five times.

Cell staining and fluorescence microscopy

Cells were double stained with May-Grunwald stain (Sigma, St. Louis, MO) and Wright-Giemsa stain (Sigma, St. Louis, MO) using standard methods. Experiments were performed in triplicate and 25 to 50 randomly selected high power fields per group were used for quantification. For visualization of cells by fluorescence microscopy, cells were fixed in 4% paraformaldehyde (JT Baker, Phillipsburg, NJ) and the actin cytoskeleton and nuclei were stained with rhodamine-phalloidin and DAPI, respectively, as described previously [16]. Wells were mounted with Vectashield (Vector Laboratories, Burlingame, CA) and examined under an Axiovert 200M fluorescent microscope (Carl Zeiss, Thornwood, NY).

Biomaterial implantation and microsphere injection *in vivo*

All procedures were performedin accordance with the regulations adopted by the NIH and approvedby the Animal Care and Use Committee of Yale University. S.C. implantations were performed essentially as described previously [20]. A total of 30 mice (C57Bl/6), age 3–4 months, were used for implantations. Each mouse received one implant (1.5×0.5 cm) in the peritoneum through a 0.7 cm incision of the skin and peritoneum. The peritoneal incision was closed with sterile sutures (silk, size 4.0), and the skin with sterile clips. To monitor macrophage accumulation, implants (3 per time point) were recovered at 1, 2, 8 and 14 days post-implantation and fixed in formalin, processed for histological analysis and stained with hematoxylin and eosin. In addition, sections were stained with Mac3 antibody to identify macrophages and FBGC as described previously [20]. Flow cytometry analysis of peritoneal lavage fluid stained with F4/80 antibody was performed to evaluate macrophage recruitment into the peritoneal cavity. Approximately 5×10^6 macrophages were detected at 48 hours post implantation. Based on the parameters of macrophage recruitment, adhesion and fusion, we

proceeded to examine the effect of phagocytosis on fusion *in vivo*. Mice were implanted with filters and divided into three groups. Two groups were injected with 5×10^7 microspheres (0.5 ml) at 0 or 48 hours following implantation. A third group received injection of vehicle (0.5 ml PBS) as a control. All mice were sacrificed at 14 days post-implantation and the implants (six per group) were cut in three segments. One set of segments was stained with DAPI and examined with the aid of an inverted microscope equipped with fluorescent optics. The remaining segments were either fixed in formalin for histological processing or embedded in OCT and used to generate cryosections in order to prevent the loss of microsphere fluorescence. Sections were viewed under an Axiovert 200M fluorescent microscope (Carl Zeiss, Thornwood, NY). Paraffin embedded sections were stained with hematoxylin and eosin and FBGC formation was quantified as described previously [20].

Statistical Analysis

All experiments were performed in triplicate (n=3) unless otherwise noted. To determine significance, Student's t-test and a Bonferroni post-hoc test were run with a 95% confidence interval.

RESULTS

IL-4 mediated fusion in monocyte/macrophage cell lines

Murine macrophage and human monocyte cell lines were grown under fusogenic conditions induced by addition of IL-4 and GM-CSF. Human monocyte cell line U937 displayed a morphological change highlighted by significant enlargement of approximately 50% of the cells, however no FBGC formation was observed (data not shown). Cell line THP-1 - also derived from human monocytes - did not display morphological change, even when exposed to the fusogenic cocktail for 15 days (not shown). Murine macrophage cell line J7746b displayed a more active response, with evident enlargement of most cells and some FBGC formation (arrows, Fig. 1C) compared to control (Fig. 1A). Similarly, RAW264.7 cells in a fusogenic environment (arrows, Fig. 1D) appeared larger than the same cells in control conditions (shown in Fig. 1B) and formed a higher number of FBGC in comparison to J7746b cells (not shown). However, overall fusion levels in these cells did not exceed 30% (Fig. 2E) and no multinucleated cells with more than 5 nuclei were observed; therefore, although these cells clearly initiated fusion, they were considered unable to undergo physiologically relevant FBGC formation.

Based on our previous observation of the dependence of primary macrophages on Rac1 activation for FBGC formation, we examined whether the same susceptibility occurred in RAW264.7 cells [25]. Inclusion of the Rac1 inhibitor NSC23766 induced a reduction in fusion (Fig. 2B) compared to control (Fig. 2A, E). We also tested the ability of RAW264.7 cells to phagocytose during fusion and found it to be similar to that of BMM (Fig. 2C). Furthermore, uptake of microspheres applied at a 10:1 sphere:cell ratio was observed concurrent with Rac1 inhibition (Fig. 2D). Enumeration of phagocytosis and fusion revealed a significant reduction in the latter in the presence of Rac inhibitor (Fig. 2E, F). In addition, exposure of RAW264.7 cells to spheres caused a reduction in overall fusion (Fig. 2E)

Phagocytic challenge via microspheres does not prevent IL-4 induced fusion *in vitro*

The reduction in fusion caused by microspheres prompted us to examine a possible effect of phagocytosis on fusion in BMM instead of RAW264.7 cells, since the latter did not display robust FBGC formation. Microspheres were added to BMM in the presence of IL-4 and GM-CSF at microsphere:cell ratios of 1:10, 1:1, and 10:1. Examination of cells during the early treatment period (1–3 days) revealed changes in cell shape, efficient uptake of spheres,

and normal fusion (not shown). At the completion of fusion (day 7), FBGC formation was evident in all wells treated with IL-4 and GM-CSF (Fig. 3B–E). The extent of fusion in cultures exposed to microspheres at 1:10 and 1:1 sphere to cell ratios appeared similar to that in cultures without spheres (Fig. 3F). Cultures exposed to microspheres at a 10:1 sphere to cell ratio displayed a trend for reduced fusion, evidenced by the presence of more single cells (Fig. 3E). However, this effect was found to be statistically insignificant (Fig. 3F).

Previously, we quantified the uptake of microspheres by BMM during fusion in the presence or absence of NSC23766 25. Specifically, we found that when exposed to microspheres at a ratio of 1:1, 70% of the BMM contained spheres at an approximate average of 3.5 spheres per cell. To expand on this finding and to distinguish possible effects of fusion on phagocytosis we quantified the number of spheres per nucleus in single BMM and FBGC. When exposed to 1:1 microsphere to cell ratio, BMM and FBGC contained 3.31 ± 1.12 and 2.98 ± 1.18 spheres/nucleus, respectively. At a ratio of 10:1, BMM and FBGC contained 7.23 ± 2.43 and 7.11 ± 4.02 spheres/nucleus, respectively. In both cases the overall uptake of spheres, expressed as average $\pm$ S.D., was similar. It should be noted however, that the number of spheres in FBGC was highly variable.

To examine the temporal specificity of the effect of phagocytosis on fusion, we repeated the experiment with BMM at a 10:1 microsphere:cell ratio and measured fusion at 3, 5, and 7 days. Enumeration of fusion, measured as the percentage of nuclei in FBGC in relation to the total number of nuclei and average number of nuclei per FBGC, revealed no significant differences at any measured time point (Fig. 3G). At day 7, percent fusion was slightly reduced, but the average number of nuclei per giant cell was similar in cultures with and without microspheres (Fig. 3H). TUNEL staining confirmed that little to no apoptosis was associated with addition of microparticles, consistent with previous reports (not shown) [26,27].

In vivo monocyte/macrophage recruitment following biomaterial implantation

In order to evaluate whether a reducing effect of phagocytosis on fusion could also be observed *in vivo*, we performed a detailed analysis of monocyte/macrophage recruitment to implantation sites and adhesion to biomaterial surfaces. We opted to utilize intra-peritoneal implantation because it allows for monitoring of cell recruitment by collection of lavage fluid. Millipore filters made of mixed cellulose ester were implanted in the peritoneal cavity of mice and the recruitment of monocytes was detected by flow cytometry with a F4/80 antibody. Analysis of samples recovered at 12 hours and at 1, 2, and 8 days following implantation revealed the progressive accumulation of monocytes (Fig. 4A). Based on the total number of cells and the estimated percent of monocytes, we concluded that there were approximately 1×10^7 monocytes in the peritoneal cavity at 48 hours. To examine the rate of adhesion of macrophages to the biomaterial surface we enumerated the number of macrophages in implant sections stained with the Mac3 antibody. Similar to the kinetics of cell recruitment revealed by flow cytometry analysis, macrophages accumulated on the surface of biomaterials in a progressive manner (Fig. 4B). In addition, examination of stained sections revealed the formation of a cell monolayer between 12 and 48 hours following implantation (Fig. 4C–E). Furthermore, FBGC formation was not detected at this time point, but was evident in day 8 implants. (Fig. 4F).

Phagocytic challenge via microspheres during the FBR does not inhibit IL-4 induced fusion *in vivo*

Based on our prior results, mice that received implants were injected with 5×10^7 microspheres into the peritoneal cavity either at the time of implantation or 48 hours later. The approximate ratio of spheres to macrophages was 10:1, matching our *in vitro* studies. At

14 days post-implantation, lavage fluid and the implants were retrieved for examination. Implants stained with DAPI revealed the presence of clusters of nuclei, indicative of FBGC formation (Fig. 5A). Examination of the same microscopic fields with the aid of a FITC filter showed extensive microsphere accumulation (Fig. 5B), which co-localized with the nuclear clusters (Fig. 5C). Lavage fluid was examined under phase contrast and revealed the presence of cells containing spheres, suggesting that phagocytosis was still ongoing (Fig. 6A, B). No FBGC were detected in lavage fluids, and the presence of free spheres was rare. Histological examination of filters indicated a FBR characterized by accumulation of cells and deposition of a collagenous capsule (Fig. 6C). FBGC formation was evident in all treatment groups. To confirm the presence of spheres at sites of high cell density, we analyzed cryosections by fluorescence. Sections were stained with DAPI to visualize nuclei and rhodamine-phalloidin to detect cytoskeletal actin. The injected microspheres contained fluorescein and were easily detected in association with the implant (Fig. 6D, E). Enumeration of FBGC per implant revealed a trend towards reduced formation in mice that received injections of spheres (Fig. 6F). However, the difference in the number of FBGC/ implant was not significant.

DISCUSSION

In the present study, we examined the effect of profuse phagocytic stimulation via microspheres on the participation of macrophage cell lines and BMM in FBGC formation via IL-4-mediated fusion. While we did observe a trend of reduced fusion correlating to increased phagocytic stimulation, it was also clear that macrophages are still capable of robust fusion even when stimulated to engage in phagocytosis in this model system. This is a potential important finding for the clinical application of implantable biomaterial devices, as this study suggests that prevention of FBGC formation *in vivo* is unlikely to be achieved by an intervention designed to invoke a phagocytic phenotype in macrophages recruited to the implant site. Rather, it appears that inhibition of the fusogenic activity of macrophages, while not impairing their phagocytic capacity, is a more promising approach. Thus, the decoupling of these two processes is critical for design of new strategies to improve implant biocompatibility, consistent with our previous findings [16].

Both fusion and phagocytosis have been shown to depend on a variety of common molecules, however, it should be noted that there are many different mechanisms by which phagocytosis occurs, depending greatly on the characteristics of the entity to be phagocytosed [9]. Similarly, macrophage fusion can be stimulated by a variety of fusogens [17–19]. We chose to utilize an IL-4 mediated fusion assay for our *in vitro* studies because of its common use in assays of FBGC in vitro and its previously characterized association with phagocytosis [8]. Polystyrene microspheres without surface functionalization were selected as a stimulus for phagocytosis for these studies because of their monodispersity, relative inertness, and reported uniform uptake by macrophages [21], all of which enable similar stimulation to each cell in a large population. Furthermore, phagocytosis of these particles in not necessarily associated with a particular receptor [21], leading to more generalizable results. Despite these careful selections, extrapolation of these results to other fusion systems and phagocytic mechanisms should be made with caution owing to the documented differences between different macrophage fusion systems [19].

Numerous studies have described both phagocytosis and fusion in monocyte and macrophage cell lines [11,18–20]. We performed a detailed examination of IL-4 mediated fusion in several cell lines and found them to be sub-optimal in comparison to BMM. In our hands, only RAW264.7 cells displayed fusion that was sensitive to a Rac1 inhibitor. This finding is consistent with our previous observations in BMM [16] and suggests that IL-4 mediated fusion is similar in primary cells and cell lines. Despite this similarity, we opted to

perform the remainder of our *in vitro* experiments with BMM due to the low overall fusion observed in RAW264.7 cell cultures. This decision was supported by recent findings of Chamberlain et al demonstrating phenotypic inequities between several murine monocyte/ macrophage cells lines and primary mouse bone marrow-derived cells [19]. Specifically, this study described significant differences in the expression of cell adhesion and activation receptors among cell lines and primary cells. In addition, the study demonstrated that cell lines displayed suboptimal cytokine expression in response to lipopolysaccharide, prompting the investigators to raise caution regarding the use of macrophage cell lines in biocompatibility studies. Our findings of reduced fusogenic capacity of several macrophage cell lines are consistent with the limited suitability of these cells in the analysis of macrophage-biomaterial interactions.

To our knowledge, this is the first study designed to rigorously evaluate the potential of a dose-dependant effect of phagocytic stimulation by microspheres on macrophage fusion. As a concept, it is intriguing to presume that macrophages that come in contact with biomaterial surfaces become frustrated by their inability to engage in phagocytosis and subsequently activate fusion-specific pathways [6]. We hypothesized that if such a mechanism existed, macrophages engaged in phagocytosis might be compelled to ignore a fusogenic stimulus. We did observe a substantial trend towards reduction in IL-4 induced fusion associated with profuse phagocytic stimulation by microspheres. The finding that BMM multinucleation is unaffected by intense phagocytic stimulation of this type indicates that the observed reduction is likely due to fewer macrophages participating in the fusion process. However, the overall findings of the present study suggest that, under normal conditions, macrophages are fully capable of fusing while engaged in phagocytosis, consistent with observations in osteoclast cultures [15]. In addition, these observations are in harmony with the notion that phagocytosis and fusion are controlled by pathways that can function independently [16]. Furthermore, we show that even in the presence of an abundant phagocytic stimulus in culture, BMM fusion still occurs at levels similar to that in conditions without a stimulus.

To confirm the relevance of our *in vitro* findings, we examined fusion in the presence of a phagocytic stimulus *in vivo*. An intraperitoneal implant model was chosen based on its extensive use in examination of macrophage function [22,28,29]. First, we determined the kinetics of macrophage adhesion and FBGC formation on the surface of a cellulose filter, a commonly used implant model for the study of FBGC formation and the FBR [20,30,31]. Additionally, to determine the number of microspheres needed to achieve a 10:1 sphere:cell ratio *in vivo*, we quantified the maximum level of macrophage recruitment following implantation. Consistent with other models of inflammation, such as peritonitis, we detected increased macrophage recruitment from 12 to 48 hours [32]. In order for the *in vivo* model to provide a concurrent phagocytic and fusogenic stimulus, it was critical to evaluate the kinetics of macrophage adhesion and fusion at the implanted biomaterial surface so that a time point at which injected microspheres would be expected to be present and acting as phagocytic stimuli to cells at the biomaterial surface prior to FBGC formation could be selected. Analysis of peritoneal lavage fluid at day 14 indicated the presence of cells containing spheres, suggesting that our injections presented a persistent phagocytic stimulus. Thus, we believe an environment was created that presented mouse peritoneal macrophages with both phagocytic and fusogenic stimuli *in vivo*. Consistent with our *in vitro* studies, we observed a trend towards reduction in fusion associated with abundant phagocytic stimulation but, overall, fusion was robust. Microspheres were also detected in the capsules surrounding implanted filters, suggesting the participation of phagocytic cells in the FBR. Thus, our *in vitro* and *in vivo* findings point towards independent, non-sequential activation of fusion and phagocytosis in macrophages participating in the FBR.

It is still not known why and how FBGC form at the surface of biomaterials. Macrophages have been shown to be extremely versatile, able to undergo phenotypic changes based on the context of their microenvironment. For example, they have been shown to differentiate into a variety of cell types including dendritic cells 33, foam cells 34, and osteoclasts 35. The latter are the closest relative to FBGC, and their formation has not been linked to phagocytosis 36. Based on our findings in this study, we conclude that BMM fusion is largely independent of phagocytosis induced by microspheres in the situation of FBGC formation at the surface of an implanted biomaterial. Supporting evidence for this assertion can be found in several elegant studies that have shown an association between FBGC formation, the surface properties of biomaterials and the presence of various proteins 37–39. Thus, macrophages are capable of detecting chemical and molecular cues with precision and reacting accordingly. Because of this impressive capacity, we conclude that exploring the decoupling of phagocytosis and fusion will yield important targets for more effective therapeutic interventions for improving biomaterial implant biocompatibility.

Acknowledgments

References

1. Anderson JM. Mechanisms of Inflammation and Infection with Implanted Devices. Cardiovascular Pathology. 1993; 2(3):S33–S41.

2. Luttikhuizen DT, Harmsen MC, Van Luyn MJ. Cellular and molecular dynamics in the foreign body reaction. Tissue Eng. 2006; 12(7):1955–70. [PubMed: 16889525]

3. Kyriakides TR, Bornstein P. Matricellular proteins as modulators of wound healing and the foreign body response. Thrombosis and Haemostasis. 2003; 90(6):986–992. [PubMed: 14652628]

4. Zhao Q, Topham N, Anderson JM, Hiltner A, Lodoen G, Payet CR. Foreign-Body Giant-Cells and Polyurethane Biostability - Invivo Correlation of Cell-Adhesion and Surface Cracking. Journal of Biomedical Materials Research. 1991; 25(2):177–183. [PubMed: 2055915]

5. Boynton EL, Henry M, Morton J, Waddell JP. The inflammatory response to particulate wear debris in total hip arthroplasty. Canadian Journal of Surgery. 1995; 38(6):507–515.

6. Anderson JM. Biological Responses to Materials. Annual Review of Materials Research. 2001; 31:81–110.

7. Anderson JM. Multinucleated Giant Cells. Current Opinion in Hematology. 2000; 7:40–47. [PubMed: 10608503]

8. Mcnally AK, DeFife KM, Anderson JM. Interleukin-4-induced macrophage fusion is prevented by inhibitors of mannose receptor activity. American Journal of Pathology. 1996; 149(3):975–985. [PubMed: 8780401]

9. Aderem A, Underhill DM. Mechanisms of phagocytosis in macrophages. Annu Rev Immunol. 1999; 17:593–623. [PubMed: 10358769]

10. Ahsan F, Rivas IP, Khan MA, Torres Suarez AI. Targeting to macrophages: role of physicochemical properties of particulate carriers--liposomes and microspheres--on the phagocytosis by macrophages. J Control Release. 2002; 79(1–3):29–40. [PubMed: 11853916]

11. McNally AK, JMA. Multinucleated giant cell formation exhibits features of phagocytosis with participation of the endoplasmic reticulum. Experimental and Molecular Pathology. 2005; 79:126–135. [PubMed: 16109404]

12. McNally AK, Jones JA, Macewan SR, Colton E, Anderson JM. Vitronectin is a critical protein adhesion substrate for IL-4-induced foreign body giant cell formation. J Biomed Mater Res A. 2008; 86(2):535–43. [PubMed: 17994558]

13. McNally AK, Macewan SR, Anderson JM. Foreign body-type multinucleated giant cell formation requires protein kinase C beta, delta, and zeta. Exp Mol Pathol. 2008; 84(1):37–45. [PubMed: 18067888]

14. Moreno JL, Mikhailenko I, Tondravi MM, Keegan AD. IL-4 promotes the formation of multinucleated giant cells from macrophage precursors by a STAT6-dependent, homotypic mechanism: contribution of E-cadherin. J Leukoc Biol. 2007; 82(6):1542–53. [PubMed: 17855502]

15. Fujikawa Y, Itonaga I, Kudo O, Hirayama T, Taira H. Macrophages that have phagocytosed particles are capable of differentiating into functional osteoclasts. Mod Rheumatol. 2005; 15(5): 346–51. [PubMed: 17029091]

16. Jay SM, Skokos E, Laiwalla F, Krady MM, Kyriakides TR. Foreign body giant cell formation is preceded by lamellipodia formation and can be attenuated by inhibition of Rac1 activation. Am J Pathol. 2007; 171(2):632–40. [PubMed: 17556592]

17. Kao WYJ, Hubbell JA. Murine macrophage behavior on peptide-grafted polyethyleneglycol-containing networks. Biotechnology and Bioengineering. 1998; 59(1):2–9. [PubMed: 10099308]

18. Godek ML, Duchsherer NL, McElwee Q, Grainger DW. Morphology and growth of murine cell lines on model biomaterials. Biomed Sci Instrum. 2004; 40:7–12. [PubMed: 15133927]

19. Chamberlain LM, Godek ML, Gonzalez-Juarrero M, Grainger DW. Phenotypic non-equivalence of murine (monocyte-) macrophage cells in biomaterial and inflammatory models. J Biomed Mater Res A. 2008

20. Kyriakides MJF, Keeney GE, Tsai A, Giachelli CM, Clark-Lewis I, Rollins BJ, Bornstein P. The CC Chemokine Ligand, CCL2/MCP1, Participates in Macrophage Fusion and Foreign Body Giant Cell Formation. American Journal of Pathology. 2004; 165(6):2157–2166. [PubMed: 15579457]

21. Tabata Y, Ikada Y. Phagocytosis of Polymer Microspheres by Macrophages. Advances in Polymer Science. 1990; 94:107–141.

22. Seymour L, Schacht E, Duncan R. The effect of size of polystyrene particles on their retention within the rat peritoneal compartment, and on their interaction with rat peritoneal macrophages in vitro. Cell Biol Int Rep. 1991; 15(4):277–86. [PubMed: 1878974]

23. Mullerad J, Cohen S, Voronov E, Apte RN. Macrophage activation for the production of immunostimulatory cytokines by delivering interleukin 1 via biodegradable microspheres. Cytokine. 2000; 12(11):1683–90. [PubMed: 11052820]

24. Gao Y, JBD, Guo F, Zheng J, Zheng Y. Rational design and characterization of a Rac GTPase-specific small molecule inhibitor. PNAS. 2004; 101(20):7618–7623. [PubMed: 15128949]

25. Jay SM, Skokos E, Laiwalla F, Krady MM, Kyriakides TR. Foreign Body Giant Cell Formation Is Preceded by Lamellipodia Formation and Can Be Attenuated by Inhibition of Rac1 Activation. Am J Pathol. 2007

26. Avital A, Shapiro E, Doviner V, Sherman Y, Margel S, Tsuberi M, Springer C. Polystyrene microspheres as a specific marker for the diagnosis of aspiration in hamsters. Am J Respir Cell Mol Biol. 2002; 27(4):511–4. [PubMed: 12356586]

27. Xing S, Santerre JP, Labow RS, Boynton EL. The effect of polyethylene particle phagocytosis on the viability of mature human macrophages. J Biomed Mater Res. 2002; 61(4):619–27. [PubMed: 12115452]

28. Tang LP, Lucas AH, Eaton JW. Inflammatory Responses to Implanted Polymeric Biomaterials - Role of Surface-Adsorbed Immunoglobulin-G. Journal of Laboratory and Clinical Medicine. 1993; 122(3):292–300. [PubMed: 8409705]

29. Keselowsky BG, Bridges AW, Burns KL, Tate CC, Babensee JE, LaPlaca MC, Garcia AJ. Role of plasma fibronectin in the foreign body response to biomaterials. Biomaterials. 2007; 28(25):3626–3631. [PubMed: 17521718]

30. Leake ES, Wright MJ, Myrvik QN. Differences in surface morphology of alveolar macrophages attached to glass and to millipore filters: a scanning electron microscope study. J Reticuloendothel Soc. 1975; 17(6):370–9. [PubMed: 1151949]

31. Nishimura M, Yuasa K, Mori K, Miyamoto N, Ito M, Tsurudome M, Nishio M, Kawano M, Komada H, Uchida A, et al. Cytological properties of stromal cells derived from giant cell tumor of bone (GCTSC) which can induce osteoclast formation of human blood monocytes without cell to cell contact. J Orthop Res. 2005; 23(5):979–87. [PubMed: 16024207]

32. Gil CD, Cooper D, Rosignoli G, Perretti M, Oliani SM. Inflammation-induced modulation of cellular galectin-1 and -3 expression in a model of rat peritonitis. Inflamm Res. 2006; 55(3):99–107. [PubMed: 16673152]

33. Matsukawa A, Kudoh S, Sano G, Maeda T, Ito T, Lukacs NW, Hogaboam CM, Kunkel SL, Lira SA. Absence of CC chemokine receptor 8 enhances innate immunity during septic peritonitis. Faseb J. 2006; 20(2):302–4. [PubMed: 16384913]

34. Shashkin P, Dragulev B, Ley K. Macrophage differentiation to foam cells. Curr Pharm Des. 2005; 11(23):3061–72. [PubMed: 16178764]

35. Li H, Cuartas E, Cui W, Choi Y, Crawford TD, Ke HZ, Kobayashi KS, Flavell RA, Vignery A. IL-1 receptor-associated kinase M is a central regulator of osteoclast differentiation and activation. J Exp Med. 2005; 201(7):1169–77. [PubMed: 15809356]

36. Vignery A. Macrophage fusion: the making of osteoclasts and giant cells. J Exp Med. 2005; 202(3):337–40. [PubMed: 16061722]

37. Kao WYJ. Evaluation of protein-modulated macrophage behavior on biomaterials: designing biomimetic materials for cellular engineering. Biomaterials. 1999; 20(23–24):2213–2221. [PubMed: 10614928]

38. McNally AK, Anderson JM. Foreign body-type multinucleated giant cell formation is potently induced by alpha-tocopherol and prevented by the diacylglycerol kinase inhibitor R59022. Am J Pathol. 2003; 163(3):1147–56. [PubMed: 12937156]

39. Jenney CR, DeFife KM, Colton E, Anderson JM. Human monocyte/macrophage adhesion, macrophage motility, and IL-4-induced foreign body giant cell formation on silane-modified surfaces in vitro. Journal of Biomedical Materials Research. 1998; 41(2):171–184. [PubMed: 9638521]
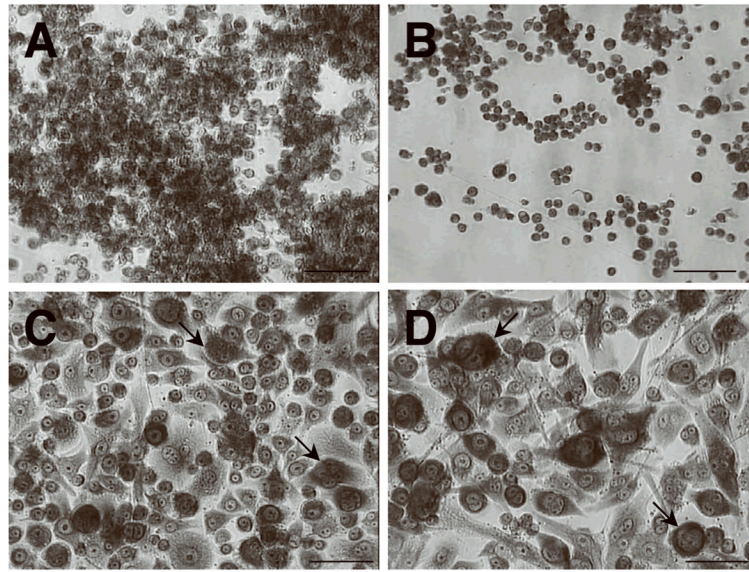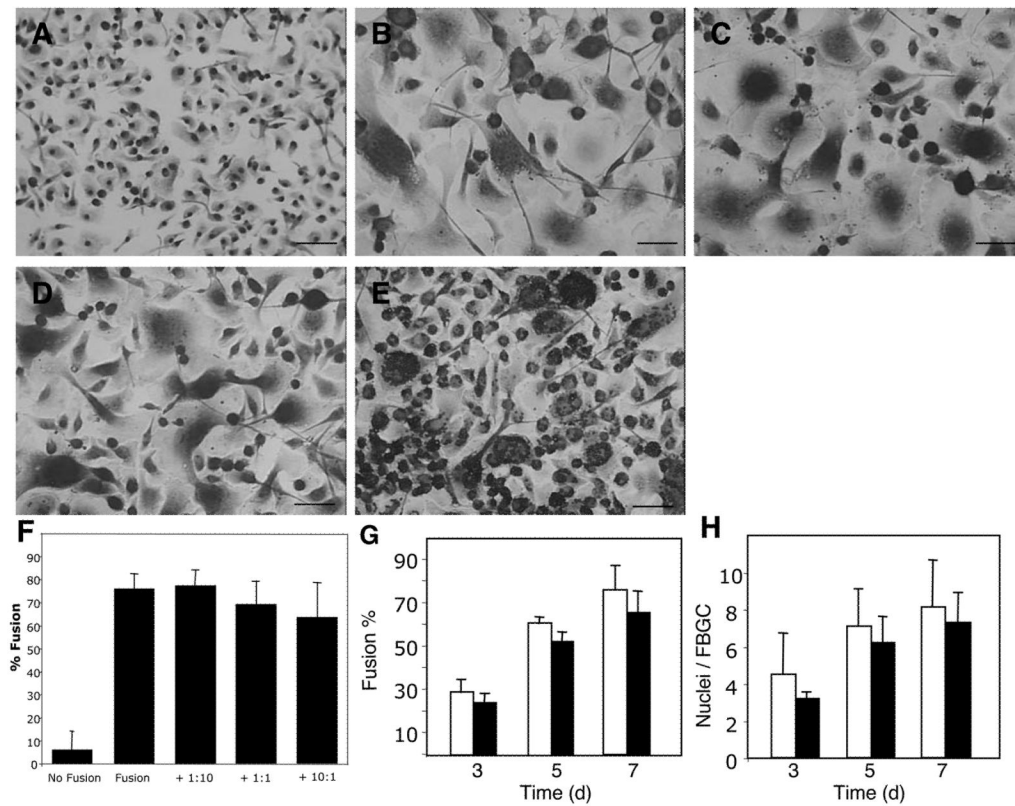
Figure 1.
Monocyte/macrophage cell lines exhibit low fusogenic potential. Representative images of Wright-Giemsa stained mouse macrophage cell lines J7746b (A) and RAW264.7 (B) under normal culture conditions. IL-4/GM-CSF treatment resulted in morphological changes in both J7746b (C) and RAW264.7 (D), however overall fusion levels were significantly lower than observed in macrophages and multinucleated cells contained, on average, 5 or less nuclei (arrows, C, D). Images are representative fields from three independent experiments. Bar = 50 μm (A–D).
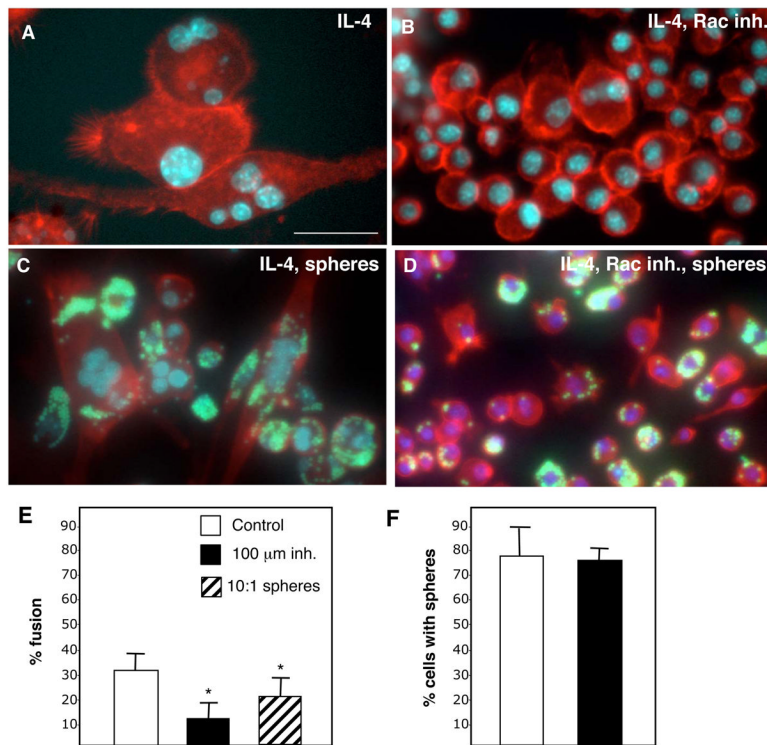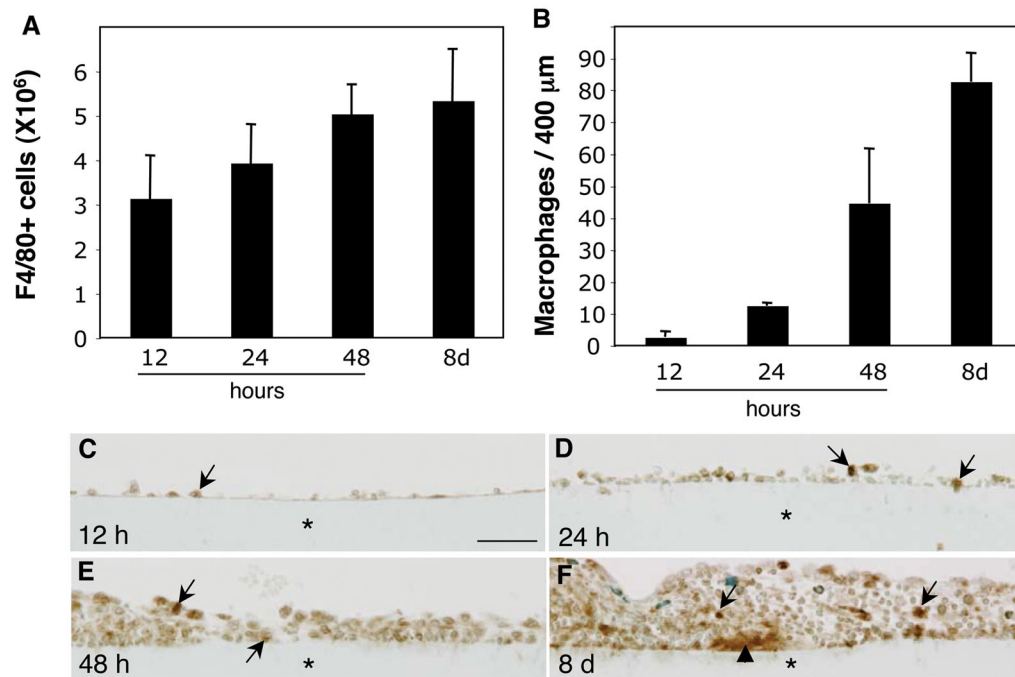
Figure 2.
Inhibition of Rac1 activation limits fusion in RAW264.7 cells. RAW264.7 cells, visualized by staining of the actin cytoskeleton with rhodamine-phalloidin (red) and nuclei with DAPI (blue) were cultured in the presence of IL-4/GM-CSF and the absence (A, C) or presence (B, D) of 25μM Rac1 inhibitor (NSC23766) for 4 days. (A) Fusion was evident at day 4, with a reduction (B) associated with Rac1 inhibition. When 3.0μm- diameter fluorescent microspheres (green) were added at a 10:1 sphere:cell ratio, phagocytosis was evident in both the absence (C) and presence (D) of NSC23766. Images are representative fields from 3 independent experiments. (E–F) Fusion and phagocytosis in RAW264.7 cells were assessed in the presence of NSC23766 and the former showed a significant reduction in fusion. Triplicate wells were prepared in 3 distinct experiments and values represent mean + S.E.M., n=3. Bar = 25 μm (A-D).
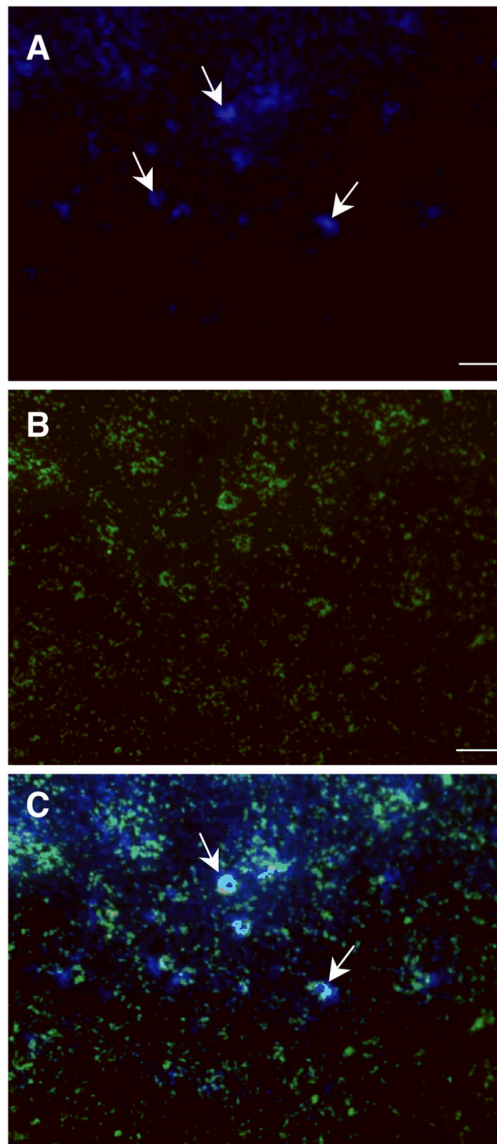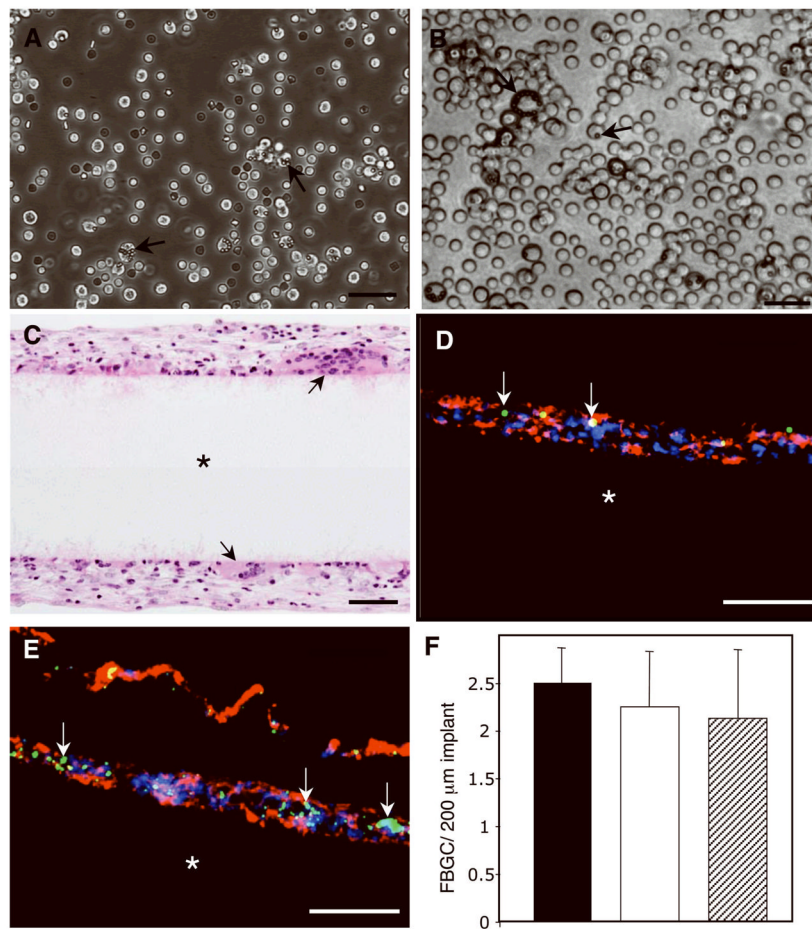
Figure 3.
Phagocytic stimulation by microspheres does not prevent fusion *in vitro* in BMM. IL-4/GM-CSF treatment (Fusion) induced significant fusion in BMM (B) compared to control (No Fusion) (A). Introduction of 3.0 μm-diameter polystyrene microspheres as phagocytic stimuli at microsphere:cell ratio of 1:10 ratio (+ 1:10), 1:1 ratio (+ 1:1), and 10:1 ratio (+ 10:1) did not cause a significant reduction in fusion (E). (G) Fusion was assessed in BMM without (white bars) or with 10:1 microspheres:cells (black bars) at 3,5, and 7 days and was not significantly reduced at any time point. (H) The average number of nuclei per giant cell was not significantly lower between the same two groups at any time point. Analysis was performed in 30 randomly selected fields per condition. Triplicate wells were prepared in 5 distinct experiments and values represent mean + S.E.M., n=5. Bar = 50 μm (A–E).

Figure 4.
Monocyte/macrophage recruitment and adhesion following biomaterial implantation. (A) Lavage fluid from the peritoneal cavity of mice implanted with Millipore filters for 12 h, and 1, 2, and 8 d was isolated and analyzed by flow cytometry for the presence of macrophages with the F4/80 antibody. (B) Sections of filters were also stained with the macrophage-specific antibody Mac 3 and the number of adherent cells was quantified (B). (C–F) Representative images of Mac-3-stained filters (*) recovered at 12 h (C), 24 h (D), 48 h (E), and 8 d (F). Immunoreactivity was detected with the peroxidase reaction (brown color) and sections were counter-stained with methyl green. Arrows in C–F, indicate adherent macrophages and arrowhead in F indicates a FBGC. n = 5. Bar = 50 μm (C–F).

Figure 5.
Microspheres co-localize with FBGC in vivo. Representative images of filters retrieved from mice 14 d following implantation and injection of 5×10^7 microspheres are shown. (A) Image of filter stained with DAPI shows accumulation of nuclei on the filter surface, including clusters indicative of FBGC formation (arrows). (B) Image of the same field showing the presence of FITC-coated microspheres. (C) Merge of A and B showing co-localization of FBGC and microspheres (arrows), n = 6. Scale bar = 100 μm (A–B).

Figure 6.
Introduction of polystyrene microspheres during the FBR does not inhibit fusion of mouse peritoneal macrophages *in vivo*. (A, B) Representative images of unfused cells from lavage fluids obtained from mice injected with microspheres at time 0 (A) and 48 h (B) are shown; arrows indicate cells with internalized spheres. (C) Representative image of H&E-stained sections from experimental (+ microspheres) implant (*) groups shows FBGC formation (arrows). (D, E) Stained cryosections (DAPI (blue nuclei), phalloidin (red, cytoskeleton) show the presence of microspheres (arrows indicate green fluorescence) near the filter surface (*). (F) The numbers of FBGC per implant after 14 days were quantified from histological images from control mice (black bar), and mice injected with spheres at time 0 (white bar) and 48 h post-implantation (hatched bar). Data was gathered from 20 randomly selected fields per implant per group and represents mean + SD; n=6. Bar = 50 μm (A–E).